

# S-wave velocity model building using PP-PS tomography with Dynamic Warping

Terence Krishnasamy\*, Ronaldo Florendo, Aravind Nangarla, Carsten Udengaard, TGS; Prajnajyoti Mazumdar, Kevin Searles, Bjorn Olofsson, ExxonMobil Technology and Engineering Company; James Gaiser, GGC-Gaiser Geophysical Consulting

## Summary

Converted wave (PS) analysis provides valuable information for subsurface characterization. It can provide information about lithology, fluid content, pore pressure, subsurface stresses and can play an important role in reservoir monitoring. Shear-wave velocity ( $V_s$ ) model building from PS data involves challenges of event registration of both the compressional wave (PP) and converted-wave (PS) data. Additionally, current deep-water ocean-bottom node acquisitions present challenges in processing converted waves due to the sparsity of the receivers optimized for PP imaging.

Presented here is a case study where we developed a workflow to build a background S-wave velocity model for an existing deep-water ocean-bottom node (OBN) survey in the Gulf of Mexico.

## Introduction

The water depth in the study area ranges from 1,768 to 1,981 m. With receiver lines deployed in a grid spacing of 426 m inline x 369 m crossline and 443 production lines with source spacing of 53.7 m x 46.5 m.

The project aimed to build a background  $V_s$  model as an input for elastic inversion. In inversion,  $V_s$  background is conventionally built using shear sonic logs recorded in wells and observed PP velocity ( $V_p$ ). Results from such seismic inversions run the risk of inaccurate subsurface characterization by ignoring the spatial variations due to changes in lithology, pressure, and subsurface stresses. One way to reduce the mentioned risk is by accounting for travel times of the PS waves travelling through the rocks as recorded on the horizontal components of the ocean bottom nodes. To expedite the work, a legacy pre-processed down-going wavefield image,  $V_p$  and associated anisotropy models were used as a starting point.

Several tomographic algorithms have been proposed to update the  $V_s$  model with various approximation and characteristics (Le Stunff et al., 2000, Berthet et al., 2001, Foss et al., 2005, Alerini et al., 2007 and D'Afonseca et al., 2014). Our approach is an extension joint PP-PS tomography

using a displacement field from dynamic warping (He et al., 2015) adapted for OBN data.

## Pre-Processing and Initial Model building

The pre-processing sequence included node positioning corrections, clock drift corrections, source signature and debubble, instrument response corrections and 3C rotation to vertical, radial, and transverse components, noise attenuation and de-multiple. The demultiple flow included removal of source-side water-layer related multiples, as well as longer period free-surface multiples, which were modelled using the down-going wavefield and adaptively subtracted from the PS radial data. S-wave splitting analysis was performed, however due to the scope of work it was decided not to pursue any s-wave splitting corrections.

The initial  $V_s$  model was built based on 3D structural extrapolation of the relationship between  $V_p$  and the  $V_p/V_s$  ratio observed at key wells. Since the dipole sonic log had no shallow coverage, the initial shallow  $V_s$  model was based on the  $V_p/V_s$  ratio obtained from a shallow PP-PS event registration using receiver stacks. Figure 1 shows the legacy  $V_p$  model, initial  $V_s$  model and the  $V_p/V_s$  ratio of the initial model. From our analysis the shallow  $V_p/V_s$  ratio was relatively high. To alleviate any possible artefacts from the Kirchhoff depth migration the  $V_p/V_s$  ratio for the first 200 m was averaged.

These initial models were used in a depth migration algorithm to generate common image gathers (CIG) for the down-going PP, as well as the PS radial data. To integrate both the P-wave down-going data and the PS radial data (upgoing wavefield just above the seabed), we created a common geometry scheme so that we can integrate these two different wavefields for the migration and velocity model building (Krishnasamy et al., 2014).

To honor lateral velocity heterogeneity, the migrated CIGs were split into eight azimuth sectors, assuming non-reciprocity. These CIGs were used in an automatic dense non-parametric residual move-out (RMO) picker to generate azimuthally sectorised RMO picks. Additionally, stacks were generated from these CIGs, for both down-going PP and PS radial data. These azimuthally sectorised stacks were used in a smooth dynamic warping algorithm (Hale 2013) to

## PP-PS tomography with Dynamic Warping

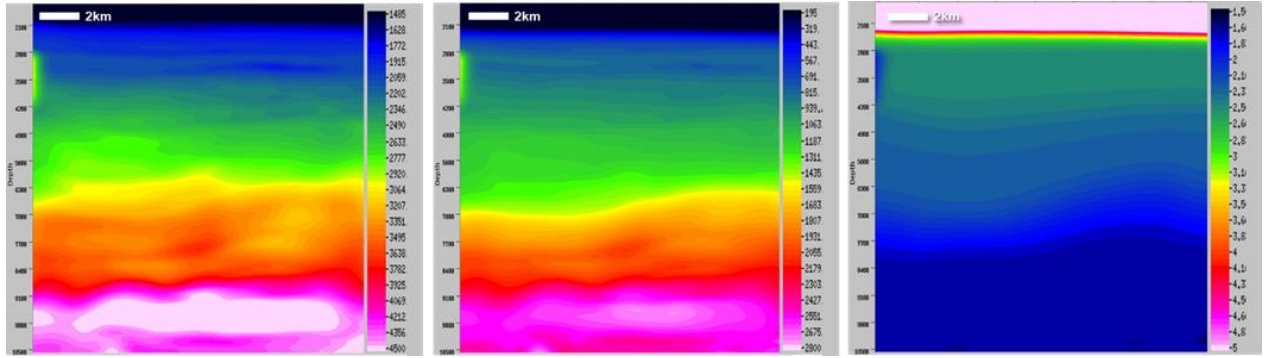


Figure 1:  $V_p$  model (left), initial  $V_s$  model (middle) and initial  $V_p/V_s$  ratio (right).

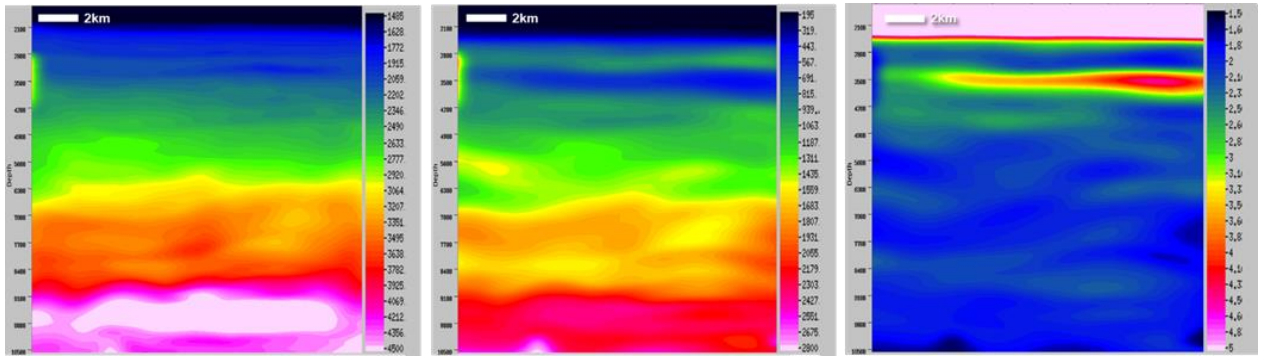


Figure 2:  $V_p$  model (left), final  $V_s$  model (middle) and resulting  $V_p/V_s$  ratio (right).

estimate displacement fields, after preconditioning, associated with the registration of PP and PS events for each azimuth sector. These displacement fields together with the RMO picks were used in a joint PP-PS tomography to obtain an updated  $V_s$  model.

### Event registration and $V_s$ model updates

Conventional tomography relies on flattening CIGs to iteratively update the velocity and anisotropy models. However, flattening the PS RMO typically does not assure correct depth registration of PP and PS events.

The objective function in the tomography is designed to reduce all residuals represented by the PP RMO, PS RMO and displacements between PP and PS events. Even though the tomography can handle all information and update all model parameters simultaneously, our tests indicate the best results are achieved with a sequence of tomographic steps where we carefully select the parameters to update. In each step, we weighted the constraints in tomography between emphasizing the reduction of RMO and registration of PP and PS events.

The  $V_p$  model was left unchanged in all our joint tomographic inversions because the model is reasonably accurate as observed from the geological depth prognosis and well tops. Thus, the PPRMO is already minimized. With that, the workflow we used can be summarized in two distinct steps. The first step involves registering PP and PS events by updating the  $V_s$  model. This was achieved by increasing the weights placed on the displacements between the PP and PS events in the tomography objective function. This process was repeated until the desired tie between PP and PS events was achieved. The second step involves running the same tomographic inversion process as described above, with weights on depth registration relaxed, thus allowing further minimization of the RMO. In this step we also allowed the epsilon field to change.

The final  $V_s$  model is shown in Figure 2. The migrated stacks for the down-going PP and the PS radial data are shown in Figure 3. Comparing these migrated images, we can see a relatively good correlation between the down going PP- and PS-migrated images. To quantify the validity of the  $V_s$  model, the displacements between PP and PS events were

## PP-PS tomography with Dynamic Warping

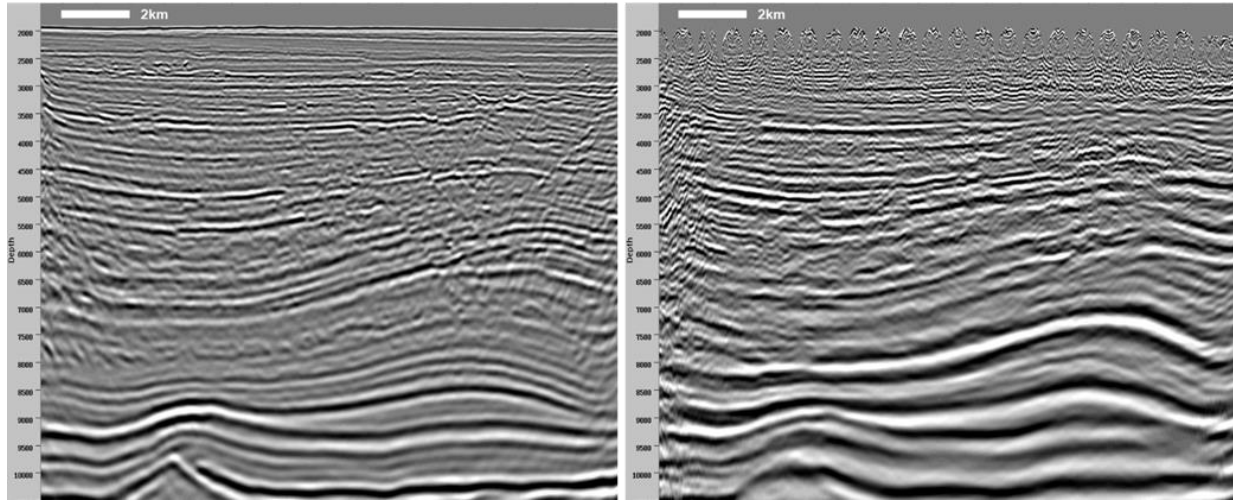


Figure 3: PP down-going Kirchhoff PSDM stack, migrated with the  $V_p$  model (left), PS Kirchhoff PSDM stack migrated with the final  $V_s$  model (right).

computed from these images for each azimuth sector. We can see that the standard deviation of the registered images is within 30 m (Figure 4). Additionally, the resulting  $V_s$  obtained from this velocity model building process is observed to correlate well with an independent pore pressure measurement in drilling operations of a borehole covered within the survey area.

### Conclusion

We built a shear wave velocity model by testing and refining a joint PP-PS velocity model building workflow on a sparse node deep water OBN survey designed for P-wave imaging.

The use of displacements between PP and PS events to update the  $V_s$  model allowed us to update the model effectively. The relatively small displacement errors between the final PP and PS events in the final  $V_s$  model, and independent geological observations in wells, indicated that the model captures the background  $V_s$  velocities relatively well.

### Acknowledgements

We thank ExxonMobil, BP and TGS for permission to publish this work.

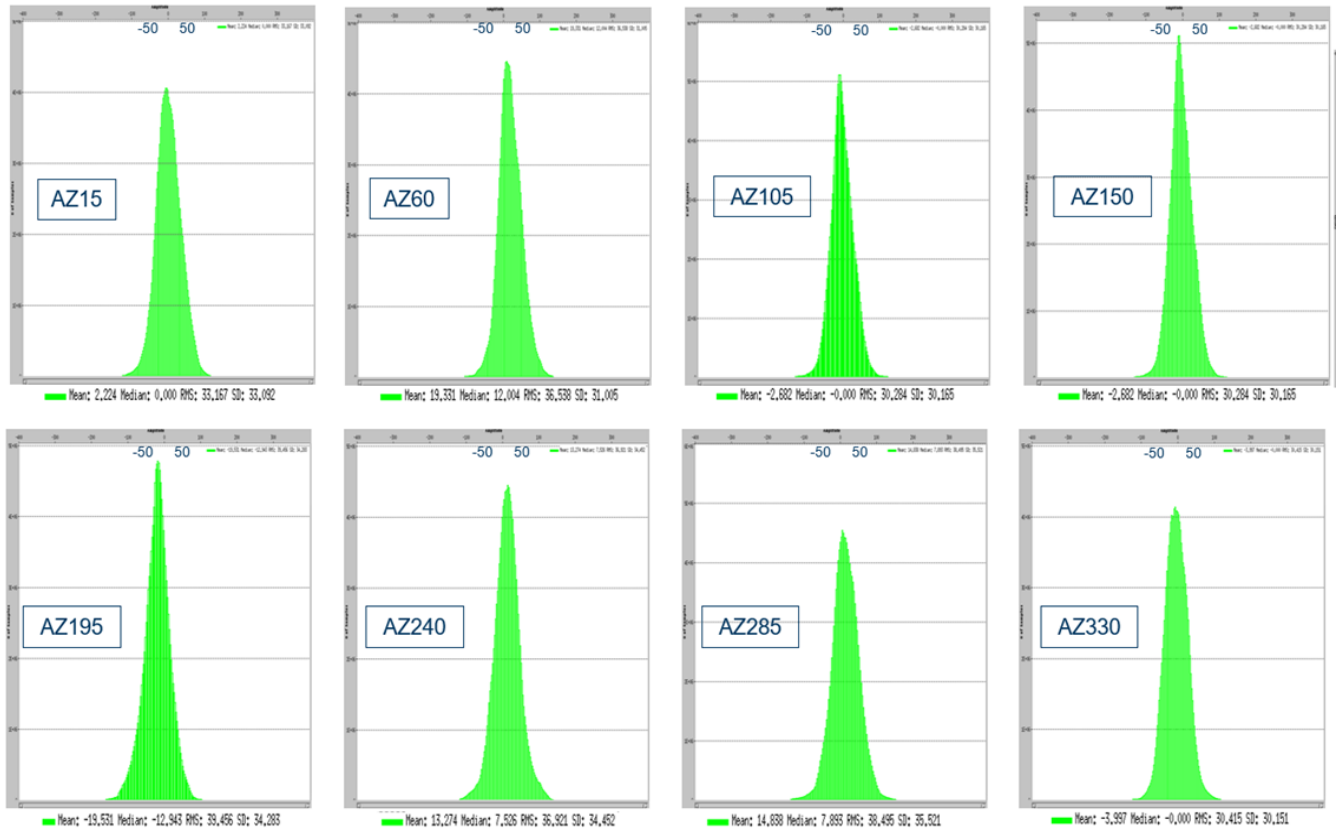


Figure 4: Event registration error/displacement histograms for the eight different azimuths used in the Vs model building computed at the zone of interest. The final displacement error that was measured is within 30m.